RSC Advances

PAPER

View Article Online
View Journal | View Issue

Published on 11 April 2016. Downloaded by Synchrotron Radiation Library on 11/09/2017 07:26:58.

Cite this: *RSC Adv.*, 2016, **6**, 35394

Highly planar thieno[3,2-*b*]thiophene-diketopyrrolopyrrole-containing polymers for organic field-effect transistors†

Xiaotong Liu,‡[ab] Jianyao Huang,‡[a] Jie Xu,[a] Dong Gao,[a] Weifeng Zhang,[a] Keli Shi[ab] and Gui Yu*[a]

Received 13th January 2016
Accepted 30th March 2016

DOI: 10.1039/c6ra01031h

www.rsc.org/advances

Two novel thieno[3,2-*b*]thiophene-flanked diketopyrrolopyrrole (TTDPP)-based copolymers PTTDPPTVT and PTTDPPSVS were designed and synthesized in order to investigate their optical, electrochemical, and morphological properties as well as device performance in organic field-effect transistors. By introducing large TTDPP units and highly π-extended moieties di(thiophen-2-yl)ethene or di(selenophen-2-yl)ethene in the conjugated backbone, the copolymers with extremely planar conjugated degree and strongly intermolecular interactions were achieved. The devices based on PTTDPPTVT and PTTDPPSVS showed hole mobilities of 0.437 and 0.067 $cm^2 V^{-1} s^{-1}$, respectively. These results demonstrated that the TTDPP unit is a promising electron deficient building block for constructing excellent performance semiconducting materials.

Introduction

Organic field-effect transistors (OFETs) have attracted significant attention because of their potential applications in electronic papers, radiofrequency identification tags, logic circuits, and sensors due to the advantages of low cost, flexibility, and large-area fabrication.[1–4] During the past few years, considerable progress has been achieved in the performance of OFETs towards the development of π-conjugated semiconductors, and some polymers with impressively excellent hole mobilities have been reported.[5–7] Furthermore, as the diversity in design of conjugated polymers continues to accelerate to meet the requirement of improving charge mobility, numerous polymer semiconductors with novel structures have been designed and synthesized. Among these polymers, diketopyrrolopyrrole (DPP)-based copolymer has emerged as a promising candidate due to their high planarity and crystallinity, which may engender superior charge transport ability and versatile applications in OFETs.[8]

To date, the optimization of the molecular structures of DPP-based copolymers has gained much attention to achieve high charge carrier mobility, and significant effects have been invested in molecular structure–property relationships for high-mobility polymer semiconductors. Many studies have proven that the high planarity of the π-conjugated backbones could enlarge the overlapping areas between π-orbitals, which enhanced the charge carrier mobility.[9,10] Moreover, the structures of the polymer backbone with excellent planarity have great influence on the molecular packing, energy levels, and crystallinity. Consequently, the investigation of backbones with good planarity is crucial to the development of high-performance DPP-based copolymers.[11] Nowadays, the DPP unit is flanked by thiophene, furan, selenophene, benzene, pyridine, and thieno[3,2-*b*]thiophene to form a conjugated donor–acceptor (D–A) molecular backbone.[7,12–17] Among these DPP-based building blocks, thiophene-flanked DPP monomers have been most widely studied with various linking moieties.[18–22] Compared with the typical thiophene monomers, thieno[3,2-*b*]thiophene (TT) contains extended π-conjugation that enhances polymer co-planarity and also promotes a more delocalized HOMO distribution along the backbone, which may result in strongly intermolecular interaction and close π–π stacking. These characteristics make the TT unit an interesting building block to be further explored for incorporating in conjugated polymers for OFETs.[16] Nevertheless, few studies towards thieno[3,2-*b*]thiophene-flanked DPP copolymers have been reported. Bronstein and co-workers firstly reported a novel thieno[3,2-*b*]thiophene-DPP (TTDPP)-based copolymer.[16] Then, a few polymers towards TTDPP unit with different branched alkyl side chains and comonomers (thiophene, selenophene, tellurophene, thiazole, and benzo[1,2-*b*:4,5-*b*′]dithiophene) have been synthesized and investigated.[23–28] However, the comonomers with highly π-extended units remain relatively unexplored for TTDPP-based copolymers. In previous research, our group have reported a superior-mobility polymer (PDVT-10)

[a]*Beijing National Laboratory for Molecular Sciences, Institute of Chemistry, Chinese Academy of Sciences, Beijing 100190, China. E-mail: yugui@iccas.ac.cn*

[b]*University of Chinese Academy of Sciences, Beijing 100049, China*

† Electronic supplementary information (ESI) available. See DOI: 10.1039/c6ra01031h

‡ These authors contributed equally to this work.

This journal is © The Royal Society of Chemistry 2016

Published on 11 April 2016. Downloaded by Synchrotron Radiation Library on 11/09/2017 07:26:58.

by incorporating a π-extended unit into thiophene-flanked DPP-based polymer backbone to extend the coplanarity and promote molecular packing.[29] Several high-performance polymers were subsequently obtained by combining other highly π-extended units including di(selenophen-2-yl)ethene (SVS) and di(thiophen-2-yl)ethene (TVT) with thiophene-flanked DPP unit in the main chain.[30–33] Inspired by the above works on thiophene-flanked DPP-based copolymers, the new design of incorporating the highly π-extended comonomers with fully planar thieno[3,2-*b*]thiophene-DPP in the backbone may have potential applications in high-performance polymer semiconductors.

Here, in order to promote the planarity and extend the conjugation length of the main chain, two new D–A type π-conjugated polymers PTTDPPTVT and PTTDPPSVS were designed and synthesized by incorporating the TTDPP as acceptor units and TVT or SVS moieties as donor units. The alkyl chains were intentionally attached in order to ensure a better solution processability. The newly designed PTTDPPTVT and PTTDPPSVS were anticipated to have strongly intermolecular interactions with short π–π stacking distance, which are capable of facilitating both intra- and intermolecular charge-carrier transport. The performance of PTTDPPTVT- and PTTDPPSVS-based OFETs was also investigated under ambient conditions with a bottom-gate/bottom-contact device configuration. As a result, the devices based on PTTDPPTVT and PTTDPPSVS showed good p-type behaviours with mobility of 0.437 and 0.067 $cm^2\ V^{-1}\ s^{-1}$, respectively. In addition, the morphological and microstructural properties of PTTDPPTVT and PTTDPPSVS thin films were also studied by atomic force microscopy (AFM) and grazing-incidence X-ray diffraction (GXRD).

Experimental

Instruments and measurement

^{1}HNMR and ^{13}C NMR spectra were recorded on a Bruker AVANCE 400 or Bruker DMX 300 spectrometer. Chemical shifts were reported as δ values [ppm] relative to internal tetramethylsilane (TMS). Electron-impact (EI) mass spectra were collected on a GCI-MS micromass (UK) spectrometer. MALDI-TOF mass spectra were collected on an Autoflex III (Bruker Daltonics Inc.) MALDI-TOF spectrometer. UV-vis-NIR absorption spectra were recorded on a Jasco-570 spectrophotometer, and the concentration of PTTDPPTVT and PTTDPPSVS in chloroform solution is 0.003 mg mL^{-1}. Molecular weights were determined with gel permeation chromatography (GPC) at 150 °C on a PL-220 system using 1,2,4-trichlorobenzene as an eluent. Fourier transform infrared spectroscopy (FT-IR) was performed on a NICOLET 6700 (Thermo Electron Corporation). Thermal gravimetric analysis (TGA) measurements were recorded using a TA Q500 instrument under a dry nitrogen flow at a heating rate of 10 °C min^{-1}. Differential scanning calorimetry (DSC) analyses were performed on a Perkin-Elmer TA-Q2000 instrument at a heating (cooling) scan rate of 5 °C min^{-1} under nitrogen atmosphere. Elemental analyses were conducted on a Flash EA 1112 elemental analyzer. AFM images of the PTTDPPTVT and PTTDPPSVS films were obtained by using a Digital Instruments Nanoscope V atomic force microscope in tapping mode. Cyclic voltammograms (CV) experiments were performed on an electrochemistry workstation (CHI660c, Chenhua Shanghai) with a three-electrode cell in a solution containing n-Bu_4NPF_6 (0.1 M) in dichloromethane. The glassy carbon electrode coated with the polymers, Pt wire and Ag/AgCl electrodes were used as the working electrode, counter electrode, and reference electrode, respectively.

Synthesis of PTTDPPTVT and PTTDPPSVS

The reagents and reactants employed were commercially available and used without any further purification unless otherwise indicated. Anhydrous tetrahydrofuran (THF) was purified with a standard distillation procedure prior to use.

2,5-Bis(2-decyltetradecyl)-3,6-bis(thieno[3,2-*b*]thiophen-2-yl)pyrrolo[3,4-*c*]pyrrole-1,4(2*H*,5*H*)-dione. This compound was synthesized according to the previously reported procedures.[16] This compound was confirmed by NMR spectroscopies (see Fig. S1 and S2†). ^{1}H NMR (300 MHz, $CDCl_3$) δ (ppm): 9.29 (s, 2H), 7.58 (d, 2H, $J = 5.1$ Hz), 7.30 (d, 2H, $J = 5.1$ Hz), 4.05 (d, 4H, $J = 7.2$ Hz), 1.99 (m, 2H), 1.20–1.32 (m, 80H), 0.83 (t, 12H); ^{13}C NMR (75 MHz, $CDCl_3$) δ (ppm): 161.67, 143.24, 140.54, 140.26, 131.98, 131.24, 127.50, 108.36, 46.57, 37.88, 31.91, 31.89, 31.23, 30.05, 29.65, 29.59, 29.53, 29.36, 29.31, 26.24, 22.66, 14.11. MALDI-TOF m/z: $[M]^+$ calcd for $C_{66}H_{104}N_2O_2S_4$, 1085.80; found, 1085.8.

3,6-Bis(5-bromothieno[3,2-*b*]thiophen-2-yl)-2,5-bis(2-decyltetradecyl)pyrrolo[3,4-*c*]pyrrole-1,4(2*H*,5*H*)-dione. To an ice-bath cooled solution of 2,5-bis(2-decyltetradecyl)-3,6-bis(thieno[3,2-*b*]thiophen-2-yl)pyrrolo[3,4-*c*]pyrrole-1,4(2*H*,5*H*)-dione (1.0 g, 0.92 mmol) in chloroform (25 mL)/DMF (1 mL) was added NBS (344.2 mg, 1.93 mmol) in batches. The mixture was stirred at this temperature for 0.5 h, warmed up to room temperature, and stirred for another 6 h until both the starting material and monobromo-substituted product disappeared by TLC monitoring. The residue was extracted with chloroform, washed with water, and dried over anhydrous $MgSO_4$. Purification on silica gel by column chromatography (petroleum ether : ethyl acetate = 5 : 1, v/v) afforded a purple solid (0.893 g, 78%). This compound was confirmed by NMR spectroscopies (see Fig. S3 and S4†). ^{1}H NMR (300 MHz, $CDCl_3$, ppm): δ 9.15 (s, 2H), 7.25 (s, 2H), 4.00 (d, 4H, $J = 7.5$ Hz), 1.92 (m, 2H), 1.19–1.29 (m, 80H), 0.81–0.88 (m, 12H); ^{13}C NMR (75 MHz, $CDCl_3$) δ (ppm): 161.42, 141.97, 140.32, 140.13, 130.43, 126.80, 122.02, 118.95, 108.33, 46.58, 37.85, 31.92, 31.89, 31.22, 30.04, 29.68, 29.65, 29.59, 29.53, 29.37, 29.32, 26.24, 22.69, 22.67, 14.12, 14.10. MALDI-TOF m/z: $[M^+]$ calcd for $C_{66}H_{102}Br_2N_2O_2S_4$, 1243.60; found, 1243.6. Anal. calcd for $C_{66}H_{102}Br_2N_2O_2S_4$: C, 63.74; H, 8.27; N, 2.25. Found: C, 63.71; H, 8.28; N, 2.22%.

General procedure for polymerization

To a 25 mL Schlenk tube was added dichalcogenophenyl ethene stannane (1 eq.), 3,6-bis(5-bromothieno[3,2-*b*]thiophen-2-yl)-2,5-bis(2-decyltetradecyl)pyrrolo[3,4-*c*]pyrrole-1,4(2*H*,5*H*)-dione (1 eq.), a certain amount of $Pd_2(dba)_3$, P(*o*-tol)$_3$, and dry toluene.

Published on 11 April 2016. Downloaded by Synchrotron Radiation Library on 11/09/2017 07:26:58.

The tube was charged with argon through a freeze–pump–thaw cycle for three times. The mixture was stirred for 12 h at 110 °C under argon atmosphere prior to pouring into a mixture of 200 mL of methanol and 15 mL of 6 M HCl (aq.). The mixture was stirred for 3 h, filtered, and the residue was then further purified by Soxhlet extraction with methanol, acetone, hexane, and dichloromethane to remove the low-molecular-weight fraction and residual catalyst. The residue was finally extracted with *o*-dichlorobenzene to afford the PTTDPPSVS and PTTDPPTVT, which were confirmed by ^{1}H NMR spectroscopies using $CDCl_3$ and deuterated 1,1,2,2-tetrachloroethane (TCE-d_2) as solvent (see Fig. S5–S8†).

Synthesis of PTTDPPTVT

Following the general procedure for polymerization, (*E*)-1,2-bis(5-(trimethylstannyl)thiophen-2-yl)ethene (M-TVT) (103.6 mg, 0.2 mmol), 3,6-bis(5-bromothieno[3,2-*b*]thiophen-2-yl)-2,5-bis(2-decyltetradecyl)pyrrolo[3,4-*c*]pyrrole-1,4(2*H*,5*H*)-dione (M-TTDPP) (248.7 mg, 0.2 mmol), $Pd_2(dba)_3$ (9 mg), P(*o*-tol)$_3$ (24.6 mg) were reacted in toluene (5 mL) for 12 h to afford a dark polymer (226.8 mg, 89%). GPC: M_n = 9.6 kDa, PDI = 1.92. ^{1}H NMR (300 MHz, $CDCl_3$) δ (ppm): 9.21 (br, 2H), 7.65–7.20 (br, 8H), 4.06 (br, 4H), 1.25 (m, 82H), 0.86 (br, 12H). FT-IR (KBr) (cm^{-1}): 3065 (aromatic), 2920, 2849 (aliphatic, C–H), 1658 (C=O), 1392 (C–N), 1543, 1463 (C=C). Anal. calcd for $C_{76}H_{108}N_2O_2S_6$: 71.65; H, 8.54; N, 2.20. Found: C, 69.73; H, 8.02; N, 2.21%.

Synthesis of PTTDPPSVS

Following the general procedure for polymerization, (*E*)-1,2-bis(5-(trimethylstannyl)selenophen-2-yl)ethene (M-SVS) (122.3 mg, 0.2 mmol), 3,6-bis(5-bromothieno[3,2-*b*]thiophen-2-yl)-2,5-bis(2-decyltetradecyl)pyrrolo[3,4-*c*]pyrrole-1,4(2*H*,5*H*)-dione (248.7 mg, 0.2 mmol), $Pd_2(dba)_3$ (9 mg), P(*o*-tol)$_3$ (24.6 mg) were reacted in toluene (5 mL) for 12 h to afford a dark polymer (238.0 mg, 87%). GPC: M_n = 11.1 kDa, PDI = 2.45. ^{1}H NMR (300 MHz, $CDCl_3$) δ (ppm): 9.27 (br, 2H), 7.65–7.20 (br, 8H), 4.06 (br, 4H), 2.60 (br, 2H), 1.25 (m, 82H), 0.86 (br, 12H). FT-IR (KBr) (cm^{-1}): 3047 (aromatic), 2920, 2849 (aliphatic, C–H), 1659 (C=O), 1392 (C–N), 1544, 1464 (C=C). Anal. calcd for $C_{76}H_{108}N_2O_2Se_2S_4$: C, 66.73; H, 7.96; N, 2.05. Found: C, 64.56; H, 7. 62; N, 2.01%.

Device fabrication

The electrical properties of OFETs were investigated using a bottom-gate bottom-contact configuration. Specifically, an n-type heavily doped Si was served as a gate electrode with a 300 nm thermally oxidized SiO_2 dielectric layer, and the gold (Au) was prepared by photolithography as source-drain electrode. The organic semiconductor films were then deposited on the surface of octadecyltrichlorosilane (OTS)-modified SiO_2/Si substrate by spin-coating from a hot *o*-dichlorobenzene solution at 1600 rpm for 1 min. Next, the prepared devices were thermally treated in the air at the annealing temperature. All the field-effect characteristics of the devices were measured by a Keithley 4200-SCS semiconductor parameter analyzer.

Results and discussion

Synthesis and thermal stability

The synthetic procedure and molecular structures of PTTDPPTVT and PTTDPPSVS are displayed in Scheme 1. The syntheses of PTTDPPTVT and PTTDPPSVS were carried out using palladium-catalyzed Stille polymerizations with $Pd_2(dba)_3$/P(*o*-tolyl)$_3$ as the catalyst in toluene. The reaction was refluxed for 12 h until the mixture turned into a gel. The structures of the two polymers were confirmed by ^{1}H NMR spectroscopies, elemental analysis, and FT-IR (shown in Fig. S9†). The elemental analysis of PTTDPPTVT and PTTDPPSVS shows a slightly lower than the expected content of carbon and hydrogen. As the result of the elemental analysis for the monomer of TTDPP is consistent with the analysis calculated value and the structures of PTTDPPTVT and PTTDPPSVS have been verified by NMR, the slightly lower value of the

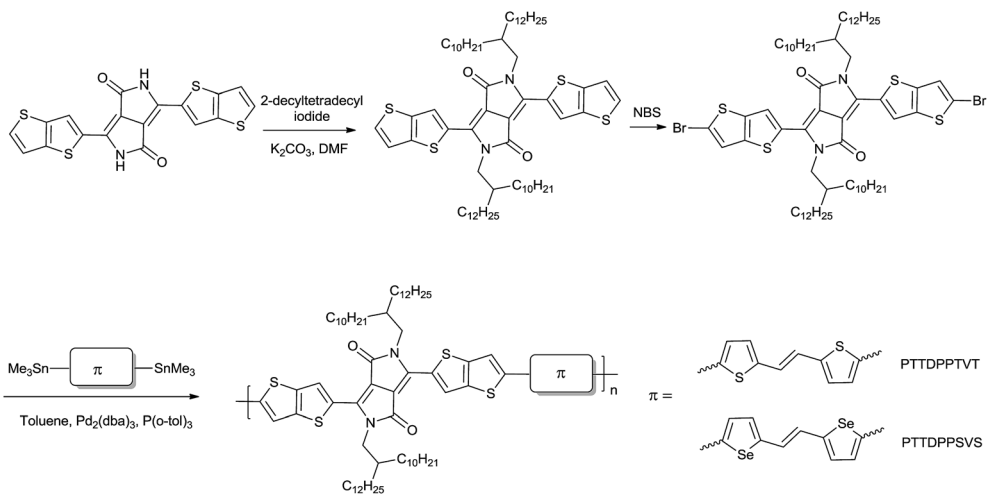

Scheme 1 Synthetic routes and molecular structures of PTTDPPTVT and PTTDPPSVS.

 This journal is © The Royal Society of Chemistry 2016

Published on 11 April 2016. Downloaded by Synchrotron Radiation Library on 11/09/2017 07:26:58.

content of carbon and hydrogen in PTTDPPTVT and PTTDPPSVS may be attributed to the existence of bromine atoms at the end groups.[34] The molecular weights of PTTDPPTVT and PTTDPPSVS were determined by GPC analysis using polystyrene standards in hot trichlorobenzene. In Fig. S10,† the number average molecular weights (M_n) of PTTDPPTVT and PTTDPPSVS were determined to be 9.6 and 11.1 kDa with a polydispersity index (PDI) of 1.92 and 2.45, respectively. The moderate molecular weights are ascribed to the highly rigid backbones of both polymers, which led to limited solubilities in the reaction. Both polymers were purified by Soxhlet extraction to remove the low-molecular-weight fraction and catalysts to circumvent detrimental effect on the intrinsic performance. The thermal properties of PTTDPPTVT and PTTDPPSVS were studied by using TGA and DSC. Both PTTDPPTVT and PTTDPPSVS exhibited excellent thermal stability with 5% weight loss at 325 and 327 °C (see Fig. S11†), respectively. In the DSC curves (Fig. S12†), no thermal transition peaks were observed for PTTDPPTVT and PTTDPPSVS in the range of 25–250 °C.

Optical, electrochemical properties, and theoretical calculations

The optical properties of the two polymers were investigated using the UV-vis-NIR absorption spectroscopy. The results of the two polymers in solution (chloroform) and in thin films are shown in Fig. 1, and the corresponding data are summarized in Table 1. PTTDPPTVT displays two absorption peaks at 448 and 686 nm in chloroform solution (shown in Fig. 1a). Similar absorption peaks of PTTDPPSVS in chloroform solution were observed at 447 and 670 nm in Fig. 1b. The absorption peaks of two polymers at short wavelength of 448 and 447 nm are attributed to π–π* transitions. And the absorption peaks at long wavelength (686 and 670 nm) of PTTDPPTVT and PTTDPPSVS are corresponding to intramolecular charge transfer arising from strong donor–acceptor interactions.[35] The maximum absorption peaks of PTTDPPTVT and PTTDPPSVS at around 680 nm were shorter than those of DPP-based copolymers at around 800 nm. We think this can result from the introduction of some π-extended units (TVT or SVS) in the backbone.[16] In Fig. 1, a small shoulder peak at around 800 nm behind a broad absorption was observed. This phenomenon was found in other DPP-based polymers, which may be the result of vibronic coupling.[28,36] In addition, red-shifts of maximum absorption and broader peaks are presented in the thin-film samples compared with those in solution, owing to the aggregation of the conjugated polymer main chains and the enhanced interchain interaction between the polymer backbones in the solid films.[37] Moreover, the absorption maximum of PTTDPPSVS shows a red-shift of 11 nm in contrast to that in solution, which may be the aggregation of the conjugated polymer in the solid films. In the case of PTTDPPTVT, a red-shift of 8 nm in solid films was also observed in contrast to that in solution. Compared to PTTDPPSVS, PTTDPPTVT exhibits a red-shifted absorption maximum of approximately 14 nm in both solution and films, which suggested that PTTDPPTVT has more effective donor–acceptor intramolecular interactions than PTTDPPSVS. The optical band gaps of PTTDPPTVT and PTTDPPSVS estimated from the absorption onset are 1.36 and 1.38 eV, respectively. The low band gaps are supposed to stem from the high molecular orbital hybridization between donor and acceptor moieties.

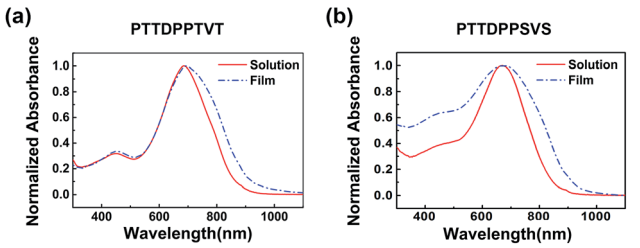

Fig. 1 UV-vis-NIR absorption spectra of PTTDPPTVT and PTTDPPSVS polymers in chloroform solution and in thin films.

The molecular energy levels of the two polymers are also important parameters for the applications in OFETs. The electrochemical cyclic voltammograms of PTTDPPTVT and PTTDPPSVS are shown in Fig. S13,† and the results are summarized in Table 1. The oxidation-onset potential (E_{ox}) and reduction onset potential (E_{red}) of PTTDPPTVT are 0.35 and −1.00 eV, which corresponds to the highest occupied molecular orbital (HOMO) and lowest unoccupied molecular orbital (LUMO) energy levels of −4.75 and −3.40 eV, respectively. The higher frontier molecular orbital energy levels of the PTTDPPTVT and PTTDPPSVS compared with TTDPP–thiophene copolymers arise from the longer effective conjugation lengths and electron-rich nature of the donor moieties.[16] For PTTDPPSVS, the values of HOMO and LUMO energy levels calculated from the values of E_{ox} and E_{red} are −4.89 and −3.44 eV, respectively. Compared with the energy levels of the PTTDPPSVS, PTTDPPTVT exhibits a higher-lying HOMO energy level whereas their LUMO levels remain almost unchanged. The electrochemical HOMO–LUMO gaps (E_g^{CV}) of PTTDPPTVT and PTTDPPSVS are 1.35 and 1.45 eV, respectively. The values are

Table 1 Optical and electrochemical properties of PTTDPPTVT and PTTDPPSVS

	λ_{max} (nm)							
Polymer	Sol	Film	E_g^{opt} (eV)	E_{red}^{onset} (eV)	E_{ox}^{onset} (eV)	E_{HOMO} (eV)	E_{LUMO} (eV)	E_g^{CV} (eV)
PTTDPPTVT	686	694	1.36	−1.00	0.35	−4.75	−3.40	1.35
PTTDPPSVS	670	681	1.38	−0.96	0.49	−4.89	−3.44	1.45

Published on 11 April 2016. Downloaded by Synchrotron Radiation Library on 11/09/2017 07:26:58.

consistent with those obtained by the optical method described above.

In order to further investigate the planarity and electronic structures of the polymers, density functional theory (DFT) calculations of the three repeating units of PTTDPPTVT and PTTDPPSVS were carried out at B3LYP/6-31G(d) level in the gas phase. All the alkyl side chains were replaced with methyl groups to avoid excessive computation demand. The optimized geometries and frontier molecular orbitals of the trimer are shown in Fig. 2. According to the optimized structures, PTTDPPTVT and PTTDPPSVS show excellent planarity along the molecular backbone direction. The torsional angles between thienothiophene–dichalcogenophenyl ethene subunits are close to 0°. In addition, both the HOMO and LUMO of the two polymers display highly delocalized π-conjugation along the polymer backbones, which facilitate intrachain carrier transport. The presence of intramolecular C–H···O hydrogen bonds (as is evident from the ^{1}H NMR spectra that the signal of β-hydrogen significantly shifted to 9.29 ppm due to the through-space deshielding effect of the carbonyl group) and profound quinoidal character of TTDPP–dichalcogenophenyl ethene are conducive to form the rigid polymer backbone with large torsional barriers.[38,39]

The OFETs performances

In order to investigate charge transport of the two polymers, the devices were fabricated with a bottom gate/bottom contact configuration. The hole mobilities of the devices were calculated by the equation: $I_{DS} = C_i\mu W(V_{GS} - V_{th})^2/2L$, where I_{DS} is the source-drain current, C_i is the capacitance of the dielectric layer, μ is the mobility of the devices, W is the width of channel, V_{GS} is the gate voltage, V_{th} is the threshold voltage of the devices, and L is the length of channel. As the annealing temperature of polymer films is an important factor for the electrical properties of the devices, the dependence of mobility on the annealing temperature was investigated. In Fig. S14,† the mobilities of the devices based on PTTDPPTVT and PTTDPPSVS first increased and then decreased with the annealing temperature increasing. The optimal annealing temperatures for PTTDPPTVT and PTTDPPSVS were 220 and 180 °C, respectively. Fig. 3 shows the transfer and output characteristics of the devices based on PTTDPPTVT and PTTDPPSVS at optimal annealing temperature, which exhibited typical p-type semiconductor behaviours. The results of mobilities and on/off current ratios of the devices based on PTTDPPTVT and PTTDPPSVS are summarized in Table 1. The max mobility and the corresponding on/off current ratio of the device based on PTTDPPSVS reach 0.067 $cm^2 V^{-1} s^{-1}$ and 5.5×10^4, respectively. The max mobility value for the films of PTTDPPTVT is 0.437 $cm^2 V^{-1} s^{-1}$, which is higher than that of PTTDPPSVS. Moreover, the average mobilities of 0.205 and 0.038 $cm^2 V^{-1} s^{-1}$ for PTTDPPTVT and PTTDPPSVS were obtained, respectively. From the data, PTTDPPTVT with thiophene units possesses higher mobility compared to that of PTTDPPSVS with selenophene units. However, some literature reported that selenophene-substitution could enhance intermolecular interaction and further promote field-effect mobility.[7] While previous studies also noticed that selenophene-substitution in copolymers caused larger π–π stacking distance due to the larger van der Waals radius of Se atoms than those of S atoms, which induces less efficient packing of polymer chains and suppresses intermolecular charge hopping.[40,41] As a consequence, the differences between mobilities of thiophene and selenophene based polymers depend on these comprehensive effects. We further investigated the morphology and microstructure of PTTDPPTVT and PTTDPPSVS to discuss the effect of selenophene-substitution (Table 2) .

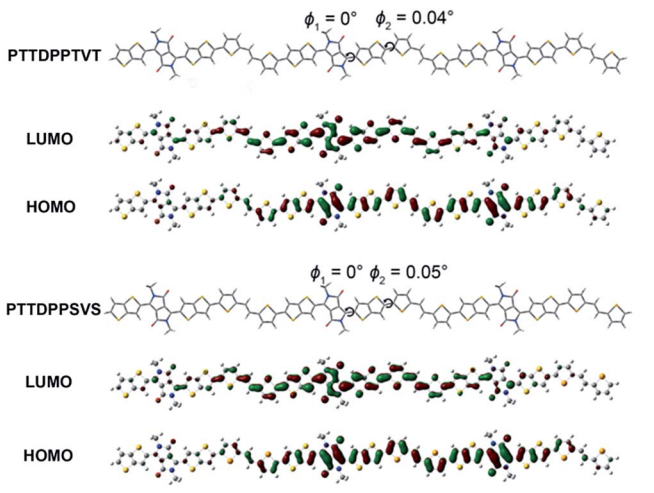

Fig. 2 DFT-optimized geometries and predicted frontier molecular orbitals of PTTDPPTVT and PTTDPPSVS trimers.

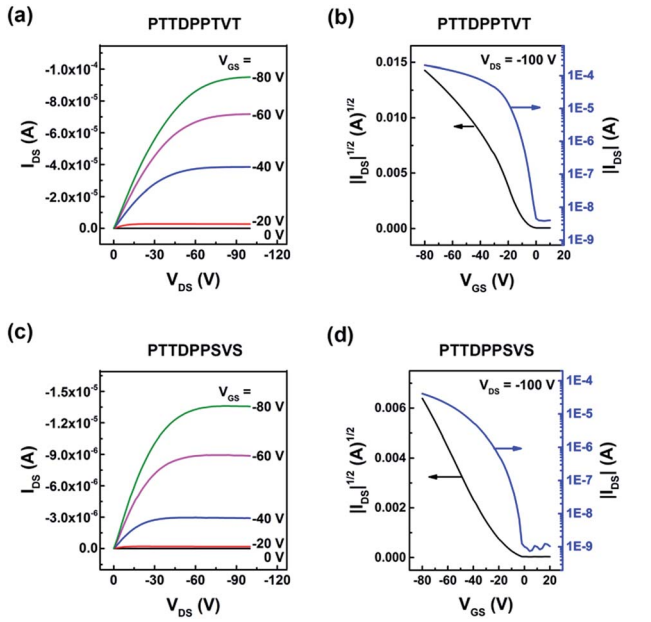

Fig. 3 Output and transfer characteristics of OFETs based on PTTDPPTVT (a and b) and PTTDPPSVS (c and d). Device dimensions: channel length L = 50 μm; channel width W = 1.4 mm.

This journal is © The Royal Society of Chemistry 2016

Published on 11 April 2016. Downloaded by Synchrotron Radiation Library on 11/09/2017 07:26:58.

Table 2 Device performances of OFETs based on PTTDPPTVT and PTTDPPSVS

	μ ($cm^2\ V^{-1}\ s^{-1}$)			
Polymer	Ave.[a]	Max.	V_{th} (V)	I_{on}/I_{off}
PTTDPPTVT	0.205	0.437	−14.0 to −3.8	10^4 to 10^6
PTTDPPSVS	0.038	0.067	−24.8 to −15.3	10^4 to 10^6

[a] The average values were calculated from 15 devices.

Morphology and microstructural characterization

The surface morphology of the PTTDPPTVT and PTTDPPSVS films was investigated by AFM and TEM. Fig. 4 shows the AFM height images of the PTTDPPTVT and PTTDPPSVS films before and after annealing at different temperatures. The aggregated granular surfaces could be observed for both polymer films. In addition, this morphological feature of the PTTDPPTVT and PTTDPPSVS films was also confirmed by TEM (Fig. S15†). After annealing to the optimal temperature, the polycrystalline grains of the PTTDPPTVT and PTTDPPSVS films grew larger than the pristine films at room temperature. When heated above the optimal annealing temperature, the PTTDPPTVT and PTTDPPSVS films became flat with smaller polycrystalline grains. It is well known that the crystallinity is favourable for efficient charge-carrier transport, and these results are in good agreement with the dependence of mobilities of PTTDPPTVT and PTTDPPSVS on thermal annealing temperatures.

In order to further investigate the crystallinity and molecular orientation of the polymer films, the GXRD were performed. The results of polymer films after thermally annealing under optimal conditions are shown in Fig. 5. In Fig. 5a and c, the two polymers reveal typical lamellar packing structures with well-developed out-of-plane Bragg peaks up to (400) and (200) in the case of PTTDPPTVT and PTTDPPSVS, respectively. The strong first-order (100) diffraction peak at 2θ of 4.9° corresponding to a d–d spacing of 18.0 Å was observed in the out-of-plane direction of the PTTDPPTVT films. In the in-plane direction, a clear π–π stacking peak at 2θ of 24.0° with the distance of 3.7 Å was obtained of the PTTDPPTVT films. For the PTTDPPSVS films, the d-spacing is calculated to be 18.4 Å due to the (100) peaks at 2θ of 4.8° and a weak π–π stacking distance of 3.8 Å at the peak of 23.2° was observed. In addition, the diffraction peaks of the PTTDPPTVT films in the out-of-plane and in-plane direction are significantly narrower and more intense compared with the ones of PTTDPPSVS, which suggested that the PTTDPPTVT film is more crystalline than PTTDPPSVS. Moreover, the smaller π–π stacking distance of the PTTDPPTVT films indicated that the presence of thiophene units results in stronger intermolecular interactions than selenophene units for these PTTDPP copolymers. As small π–π distance and strong crystallinity largely contributed to good performance in charge transport, higher mobility was obtained with the devices based on PTTDPPTVT compared with that of PTTDPPSVS.

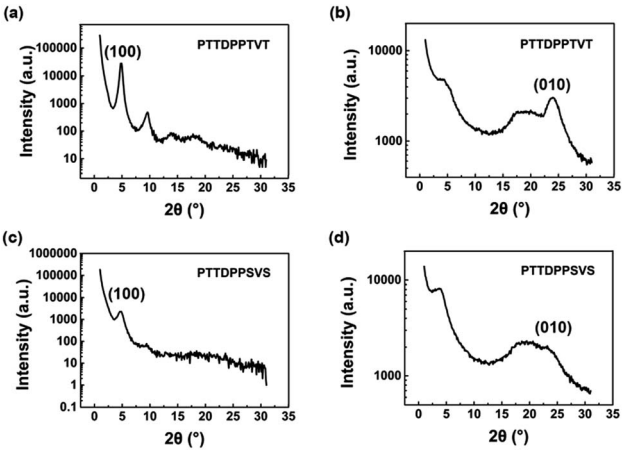

Fig. 5 Grazing incidence X-ray diffraction pattern (out of plane) of PTTDPPTVT (a) and PTTDPPSVS thin films (c) on the OTS-modified SiO_2/Si substrates annealed at optimal temperatures. In-plane X-ray diffraction pattern of PTTDPPTVT (b) and PTTDPPSVS (d) on the OTS-modified SiO_2/Si substrates annealed at optimal temperatures.

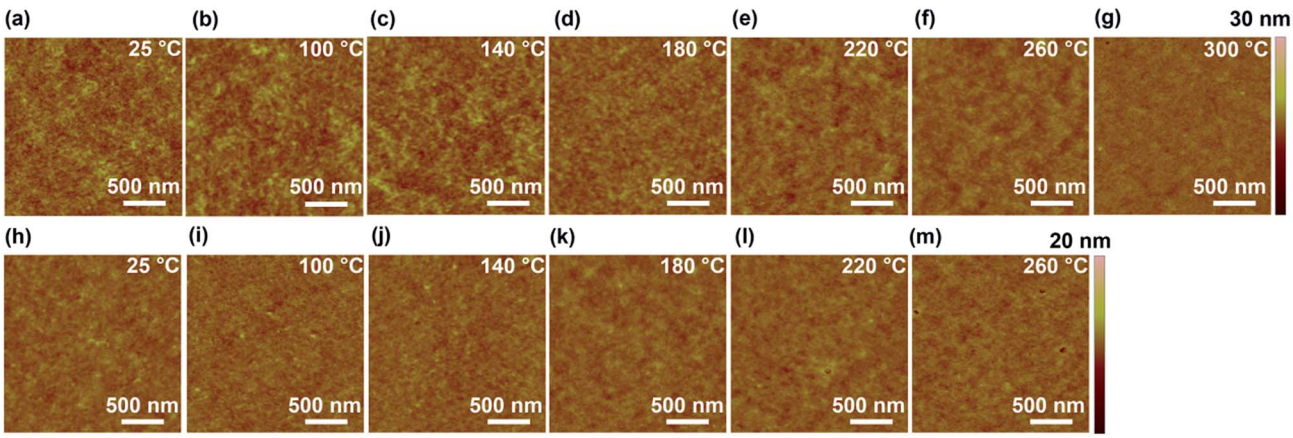

Fig. 4 AFM height images of polymer films on OTS-modified SiO_2/Si substrates. The PTTDPPTVT thin films: without annealing (a), and with annealing at 100, 140, 180, 220, 260, and 300 °C (b–g). The PTTDPPSVS thin films: without annealing (c), and with annealing at 100, 140, 180, 220, and 260 °C (h–m).

Published on 11 April 2016. Downloaded by Synchrotron Radiation Library on 11/09/2017 07:26:58.

Conclusions

Two new D–A copolymers composed of highly π-extended TVT or SVS as donor units and TTDPP as acceptor units were synthesized and well characterized. Both the copolymers possess good solubility, low bandgap and short π–π stacking distance for effective charge transport. The two polymers were characterized under ambient conditions with bottom-gate/bottom-contact device configurations. Mobility of 0.437 $cm^2 V^{-1} s^{-1}$ with current on/off current ratio of 5.3×10^4 was obtained from the PTTDPPTVT thin film. For PTTDPPSVS, a lower mobility of 0.067 $cm^2 V^{-1} s^{-1}$ with corresponding on/off current ratio of 5.5×10^4 was achieved. Furthermore, the morphology and microstructure of these films were characterized by GXRD and AFM. The results showed that the PTTDPPTVT films exhibit enhanced degree of crystallinity and shorter π–π stacking distance compared with PTTDPPSVS, which gave rise to the higher mobility of the devices based on PTTDPPTVT. Our study in this work clearly shows that PTTDPP unit is a potential candidate building block for achieving highly planar conjugated materials in the applications of OFETs.

Acknowledgements

This work was financially supported by the Strategic Priority Research Program of the Chinese Academy of Sciences (XDB12030100) and the National Natural Science Foundation of China (21474116 and 51233006). The GXRD results were tested at 1W1A (Beijing Synchrotron Radiation Facility), 23A1 Station of National Synchrotron Radiation Research Center (NSRRC, Taiwan), and BL16B1 Station of Shanghai Synchrotron Radiation Facility (SSRF). The authors gratefully thank the assistance of scientists from the stations during the experiments.

Notes and references

1 M. Kaltenbrunner, T. Sekitani, J. Reeder, T. Yokota, K. Kuribara, T. Tokuhara, M. Drack, R. Schwodiauer, I. Graz, S. Bauer-Gogonea, S. Bauer and T. Someya, *Nature*, 2013, **499**, 458.

2 B. Crone, A. Dodabalapur, Y. Y. Lin, R. W. Filas, Z. Bao, A. LaDuca, R. Sarpeshkar, H. E. Katz and W. Li, *Nature*, 2000, **403**, 521.

3 H. U. Khan, M. E. Roberts, O. Johnson, R. Forch, W. Knoll and Z. Bao, *Adv. Mater.*, 2010, **22**, 4452.

4 L. P. Wang, X. D. Xie, S. W. Shi, K. L. Shi, Z. P. Mao, W. F. Zhang, H. Q. Wang and G. Yu, *Polymer*, 2015, **68**, 302.

5 X. Liu, Y. Guo, Y. Ma, H. Chen, Z. Mao, H. Wang, G. Yu and Y. Liu, *Adv. Mater.*, 2014, **26**, 3631.

6 J. Li, Y. Zhao, H. S. Tan, Y. Guo, C. A. Di, G. Yu, Y. Liu, M. Lin, S. H. Lim, Y. Zhou, H. Su and B. S. Ong, *Sci. Rep.*, 2012, **2**, 754.

7 I. Kang, H. J. Yun, D. S. Chung, S. K. Kwon and Y. H. Kim, *J. Am. Chem. Soc.*, 2013, **135**, 14896.

8 Y. Li, P. Sonar, L. Murphy and W. Hong, *Energy Environ. Sci.*, 2013, **6**, 1684.

9 B. Nketia-Yawson, H. S. Lee, D. Seo, Y. Yoon, W. T. Park, K. Kwak, H. J. Son, B. Kim and Y. Y. Noh, *Adv. Mater.*, 2015, **27**, 3045.

10 L. Fu, W. Fu, P. Cheng, Z. Xie, C. Fan, M. Shi, J. Ling, J. Hou, X. Zhan and H. Chen, *J. Mater. Chem. A*, 2014, **2**, 6589.

11 J. S. Lee, S. K. Son, S. Song, H. Kim, D. R. Lee, K. Kim, M. J. Ko, D. H. Choi, B. Kim and J. H. Cho, *Chem. Mater.*, 2012, **24**, 1316.

12 T. J. Ha, P. Sonar and A. Dodabalapur, *ACS Appl. Mater. Interfaces*, 2014, **6**, 3170.

13 B. Sun, W. Hong, Z. Yan, H. Aziz and Y. Li, *Adv. Mater.*, 2014, **26**, 2636.

14 M. Shahid, T. McCarthy-Ward, J. Labram, S. Rossbauer, E. B. Domingo, S. E. Watkins, N. Stingelin, T. D. Anthopoulos and M. Heeney, *Chem. Sci.*, 2012, **3**, 181.

15 W. Li, T. Lee, S. J. Oh and C. R. Kagan, *ACS Appl. Mater. Interfaces*, 2011, **3**, 3874.

16 H. Bronstein, Z. Chen, R. S. Ashraf, W. Zhang, J. Du, J. R. Durrant, P. S. Tuladhar, K. Song, S. E. Watkins, Y. Geerts, M. M. Wienk, R. A. Janssen, T. Anthopoulos, H. Sirringhaus, M. Heeney and I. McCulloch, *J. Am. Chem. Soc.*, 2011, **133**, 3272.

17 S. Shi, X. Xie, R. Qu, S. Chen, L. Wang, M. Wang, H. Wang, X. Li and G. Yu, *RSC Adv.*, 2013, **3**, 18944.

18 Y. Xiong, X. Qiao and H. Li, *Polym. Chem.*, 2015, **6**, 6579.

19 P. Pattanasattayavong, M. Sygletou, E. Kymakis, E. Stratakis, F. Yan, V. G. Gregoriou, T. D. Anthopoulos and C. L. Chochos, *RSC Adv.*, 2014, **4**, 58404.

20 M. J. Cho, J. Shin, T. R. Hong, H. A. Um, T. W. Lee, G. W. Kim, J. H. Kwon and D. H. Choi, *Polym. Chem.*, 2015, **6**, 150.

21 J. C. Bijleveld, R. A. M. Verstrijden, M. M. Wienk and R. A. J. Janssen, *J. Mater. Chem.*, 2011, **21**, 9224.

22 H. Chen, Y. Guo, Z. Mao, D. Gao and G. Yu, *J. Polym. Sci., Part A: Polym. Chem.*, 2014, **52**, 1970.

23 J. Shin, G. E. Park, D. H. Lee, H. A. Um, T. W. Lee, M. J. Cho and D. H. Choi, *ACS Appl. Mater. Interfaces*, 2015, **7**, 3280.

24 H. Bronstein, E. Collado-Fregoso, A. Hadipour, Y. W. Soon, Z. Huang, S. D. Dimitrov, R. S. Ashraf, B. P. Rand, S. E. Watkins, P. S. Tuladhar, I. Meager, J. R. Durrant and I. McCulloch, *Adv. Funct. Mater.*, 2013, **23**, 5647.

25 R. S. Ashraf, I. Meager, M. Nikolka, M. Kirkus, M. Planells, B. C. Schroeder, S. Holliday, M. Hurhangee, C. B. Nielsen, H. Sirringhaus and I. McCulloch, *J. Am. Chem. Soc.*, 2015, **137**, 1314.

26 I. Meager, R. S. Ashraf, S. Mollinger, B. C. Schroeder, H. Bronstein, D. Beatrup, M. S. Vezie, T. Kirchartz, A. Salleo, J. Nelson and I. McCulloch, *J. Am. Chem. Soc.*, 2013, **135**, 11537.

27 K. Tandy, G. K. Dutta, Y. Zhang, N. Venkatramaiah, M. Aljada, P. L. Burn, P. Meredith, E. B. Namdas and S. Patil, *Org. Electron.*, 2012, **13**, 1981.

28 I. Meager, R. S. Ashraf, S. Rossbauer, H. Bronstein, J. E. Donaghey, J. Marshall, B. C. Schroeder, M. Heeney, T. D. Anthopoulos and I. McCulloch, *Macromolecules*, 2013, **46**, 5961.

 This journal is © The Royal Society of Chemistry 2016

Published on 11 April 2016. Downloaded by Synchrotron Radiation Library on 11/09/2017 07:26:58.

29 H. Chen, Y. Guo, G. Yu, Y. Zhao, J. Zhang, D. Gao, H. Liu and Y. Liu, *Adv. Mater.*, 2012, **24**, 4618.
30 J. Shin, T. R. Hong, T. W. Lee, A. Kim, Y. H. Kim, M. J. Cho and D. H. Choi, *Adv. Mater.*, 2014, **26**, 6031.
31 I. Kang, T. K. An, J. A. Hong, H. J. Yun, R. Kim, D. S. Chung, C. E. Park, Y. H. Kim and S. K. Kwon, *Adv. Mater.*, 2013, **25**, 524.
32 J. Y. Back, H. Yu, I. Song, I. Kang, H. Ahn, T. J. Shin, S.-K. Kwon, J. H. Oh and Y.-H. Kim, *Chem. Mater.*, 2015, **27**, 1732.
33 Y. R. Cheon, Y. J. Kim, J.-J. Ha, M.-J. Kim, C. E. Park and Y.-H. Kim, *Macromolecules*, 2014, **47**, 8570.
34 G. Zhang, K. Liu, Y. Li and M. Yang, *Polym. Int.*, 2009, **58**, 665.
35 Z. Zeng, Y. Li, J. Deng, Q. Huang and Q. Peng, *J. Mater. Chem. A*, 2014, **2**, 653.
36 X. Zhang, L. J. Richter, D. M. DeLongchamp, R. J. Kline, M. R. Hammond, I. McCulloch, M. Heeney, R. S. Ashraf, J. N. Smith, T. D. Anthopoulos, B. Schroeder, Y. H. Geerts, D. A. Fischer and M. F. Toney, *J. Am. Chem. Soc.*, 2011, **133**, 15073.
37 T. K. An, I. Kang, H.-J. Yun, H. Cha, J. Hwang, S. Park, J. Kim, Y. J. Kim, D. S. Chung, S.-K. Kwon, Y.-H. Kim and C. E. Park, *Adv. Mater.*, 2013, **25**, 7003.
38 N. E. Jackson, B. M. Savoie, K. L. Kohlstedt, M. Olvera de la Cruz, G. C. Schatz, L. X. Chen and M. A. Ratner, *J. Am. Chem. Soc.*, 2013, **135**, 10475.
39 N. E. Jackson, K. L. Kohlstedt, B. M. Savoie, M. Olvera de la Cruz, G. C. Schatz, L. X. Chen and M. A. Ratner, *J. Am. Chem. Soc.*, 2015, **137**, 6254.
40 Z. Zhang and Y. Qin, *ACS Macro Lett.*, 2015, **4**, 679.
41 K. H. Park, K. H. Cheon, Y. J. Lee, D. S. Chung, S. K. Kwon and Y. H. Kim, *Chem. Commun.*, 2015, **51**, 8120.